Switching Notes

Note 31

15 January 2002

Some Considerations for Multichannel Switching

Carl E. Baum and Jane M. Lehr

Air Force Research Laboratory
Directed Energy Directorate

Abstract

This paper explores some techniques for use in multichannel switching. These techniques are concerned with minimizing the effect of one in N switches firing in turn reducing the voltages on the remaining switches and thereby delaying or preventing the closure of some or all of these. The techniques include a bifilar choke, dividing a transmission line into N such each with N times the characteristic impedance to achieve transit-time isolation, and the effect of an N-fold rotation axis. Detailed consideration is then given to an N-conductor transmission line with this symmetry to obtain some measure of the quantitative improvement.

This work was sponsored in part by the Air Force Office of Scientific Research, and in part by the Air Force Research Laboratory, Directed Energy Directorate.

1. Introduction

This paper explores some techniques, which may be useful for multichannel switching. The reader is referred to [4] for an extensive discussion of multichannel switching, which need not be repeated here.

The general problem of multichannel switching concerns the fact that, if some one out of say N switches (or arc channels) closes before another, then the voltage across the latter gap is decreased before it closes, perhaps resulting in the failure of the latter gap to close at all. This is related to the switch jitter or uncertainty as to the time a switch will close after the application of an excitation (voltage) waveform.

The problem then is one of *electrical isolation* from one switch gap to its nearest-neighbor switch(es). This can be achieved by:

$$\left.\begin{matrix}\text{transit-time isolation}\\ \text{impedance isolation}\end{matrix}\right\} = \text{electrical isolation} \tag{1.1}$$

The first is achieved by physical separation, including forcing signals from gap to another to take a nondirect route (nonstraight path). The second concerns making the signal strength reaching a second gap from a first small because of the impedance associated with the path between the two, such as by increased inductance and lowered capacitance.

Besides isolation of one switch from another, there is another reason to have all the switches fire at nearly the same time. If one wishes the risetime (or, better, t_{mr}, the peak voltage divided by the peak time derivative) to be as small as possible, then it is necessary that all, or nearly all, of the switches fire within a time window smaller than the risetime (calculated as if all switches fired simultaneously). This is again the problem of switch jitter, or better the problem of *switch spread.* By spread we mean the time difference between first and last of N switches firing. If N is large, one can relax this to the time window during which some very large fraction (say 90% or whatever) of the switches fire. Since jitter is typically defined in terms of a standard deviation of the firing times, it is considerably smaller than the important term: *spread.* Note that in some applications (e.g., a timed array antenna [2]) it is desired to have the switches fire in some preprogrammed progression and spread needs to be defined in terms of a time window about this set of preprogrammed times.

2. Mutual Inductance (Bifilar Choke) to Increase Voltage on Lagging Spark Gap

When one switch fires it tends to lower the voltage across an adjacent switch. One would like to be able to instead increase the voltage across the second switch. One way to do this is via a bifilar choke, a special kind of transformer, as illustrated in Fig. 2.1. The basic idea is that the two currents, if equal, link no net flux in the transformer core, giving negligible impedance to the common-mode current. If, however, only one gap is closed the transformer core presents a large impedance to this current and increases the voltage on the second switch. While this is illustrated with a magnetic core (e.g., ferrite), one can also have an air (or dielectric) core with the two wires as helices with a common axis but with opposite pitch angles two make two equal currents give zero net magnetic flux. Note that, in opposite sense to the usual bifilar choke, which presents a large impedance to the common mode, this one presents a large impedance to the differential mode.

To analyze this problem consider the impedance matrices presented to the voltages and currents. For the transformer we have

$$\left(\tilde{V}_n^{(1)}(s) - \tilde{V}_n^{(2)}(s)\right) = s\left(L_{n,m}\right) \cdot \left(\tilde{I}_n(s)\right)$$
$$\left(L_{n,m}\right) = \begin{pmatrix} L & M \\ M & L \end{pmatrix}$$
$$L^2 - M^2 \geq 0 \text{ (positive semidefine matrix)}$$
$$\sim \equiv \text{two-sided Laplace transform} \qquad (2.1)$$
$$s \equiv \text{Laplace-transform variable}$$

One defines the coupling coefficient by

$$k = \frac{M}{L} \quad , \quad |k| \leq 1 \quad , \quad \left(L_{n,m}\right) = L\begin{pmatrix} 1 & k \\ k & 1 \end{pmatrix} \qquad (2.2)$$

Note that M can be positive or negative. For our case of interest we want minimal voltage drop for $I_1 = I_2$, so we take *M negative.*

The switch impedance matrix is diagonal as

$$\left(\tilde{Z}_{n,m}^{(s)}(s)\right) = \begin{pmatrix} \tilde{Z}_1^{(s)}(s) & 0 \\ 0 & \tilde{Z}_2^{(s)}(s) \end{pmatrix} = \left(\tilde{Y}_{n,m}^{(s)}(s)\right)^{-1} = \begin{pmatrix} \tilde{Y}_1^{(s)}(s) & 0 \\ 0 & \tilde{Y}_2^{(s)}(s) \end{pmatrix}^{-1} \qquad (2.3)$$

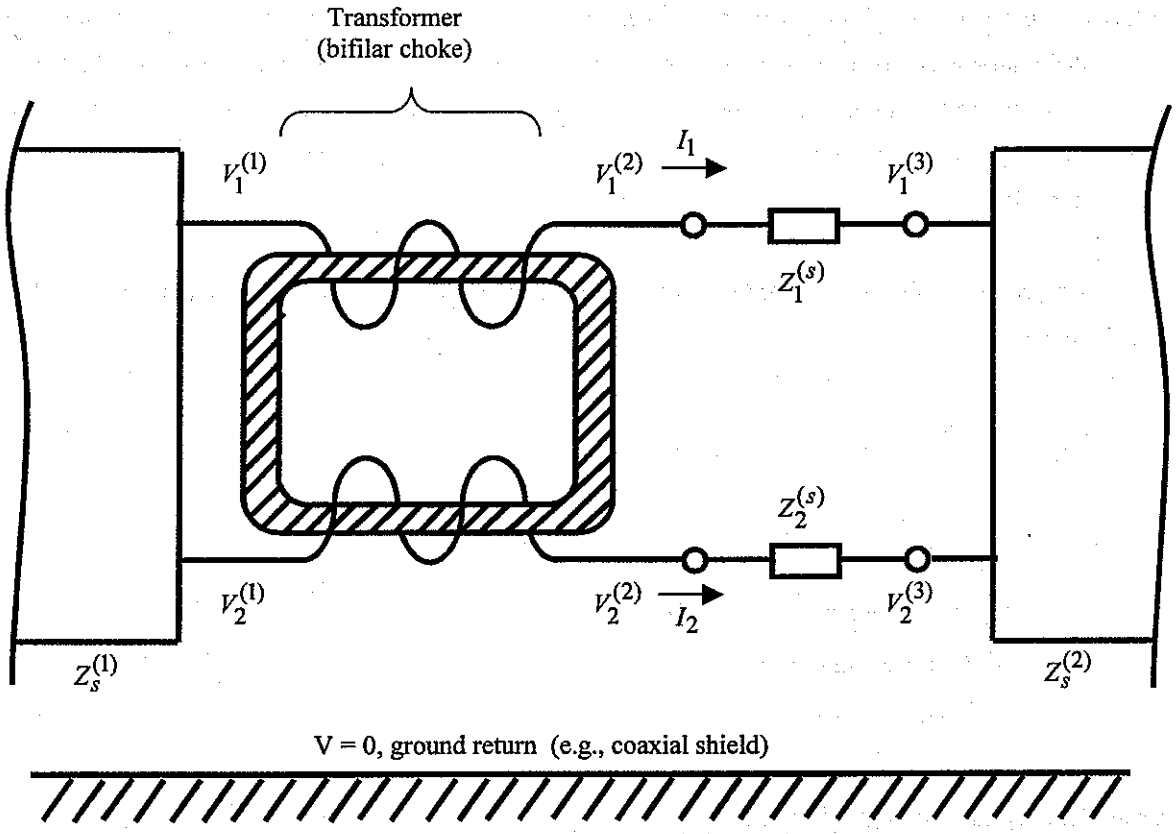

Fig. 2.1 Bifilar Choke

This does not apply to general time varying inductance and resistance, so we will use it with simplifying assumptions. This is used in

$$\left(\tilde{V}_n^{(2)}(s)\right) - \left(\tilde{V}_n^{(3)}(s)\right) = \left(\tilde{Z}_{n,m}^{(s)}(s)\right) \cdot \left(\tilde{I}_n(s)\right) = \begin{pmatrix} \tilde{Z}_1^{(s)}(s) & \tilde{I}_1(s) \\ \tilde{Z}_2^{(s)}(s) & \tilde{I}_2(s) \end{pmatrix} \tag{2.4}$$

Consider an important special case:

$$\begin{aligned} &\tilde{Z}_2^{(s)}(s) = \infty \text{ (open circuit)} \\ &\tilde{Z}_1^{(s)}(s) = 0 \text{ (short circuit)} \\ &\tilde{I}_2(s) = 0 \\ &V_1^{(3)} = V_1^{(2)} \\ &\tilde{V}_1^{(1)}(s) - \tilde{V}_1^{(3)}(s) = sL\tilde{I}_1(s) \text{ (making } I_1 \text{ small)} \\ &\tilde{V}_2^{(1)}(s) - \tilde{V}_2^{(2)}(s) = s\,M\,\tilde{I}_1(s) \end{aligned} \tag{2.5}$$

Setting

$$\left(\tilde{V}_n^{(1)}\right) = \tilde{V}^{(1)}(s)\begin{pmatrix}1\\1\end{pmatrix} \quad , \quad \left(\tilde{V}_n^{(3)}(s)\right) = \tilde{V}^{(3)}(s)\begin{pmatrix}1\\1\end{pmatrix} \tag{2.6}$$

we have

$$\begin{aligned} &\tilde{V}_2^{(2)}(s) - \tilde{V}^{(3)}(s) = s\left[L-M\right]\tilde{I}_1(s) = s\,L\left[1-k\right]\tilde{I}_1(s) \\ &\frac{\tilde{V}_2^{(2)}(s) - \tilde{V}^{(3)}(s)}{\tilde{V}^{(1)}(s) - \tilde{V}^{(3)}(s)} = 1-k \end{aligned} \tag{2.7}$$

Since k is negative and nearly –1 the voltage across the second gap has been almost *doubled* instead of being decreased. Of course, this assumes that there has been a negligible change in $V^{(1)}$ and $V^{(3)}$ in the process. This is the case for small I_1 which applies for times of interest if L is sufficiently large and/or the source and load impedances are sufficiently small.

At the same time that L should be large, L + M should be small so that if both switches close

$$\left[\tilde{V}^{(1)}(s) - \tilde{V}^{(3)}(s)\right]\begin{pmatrix}1\\1\end{pmatrix} = s\left(L_{n,m}\right) \cdot \left(\tilde{I}_n(s)\right)$$

$$\tilde{I}_1(s) = \tilde{I}_2(s) \quad , \quad \tilde{I}(s) \equiv \tilde{I}_1(s) + \tilde{I}_2(s) \quad \text{(common mode)} \tag{2.8}$$

$$\tilde{V}^{(1)}(s) - \tilde{V}^{(3)}(s) = s\frac{L+M}{2}\tilde{I}(s) = sL\frac{1+k}{2}\tilde{I}(s)$$

and $sL[1+k]/2$ is sufficiently small compared to source and load impedance for high frequencies (or early times) of interest. So we need small $|\ 1\text{-}k\ |$.

Having seen what can be done for two switches, the technique can be extended by bifurcating each switch, i.e., by replacing each switch with two switches plus a bifilar choke. This results in four switches and three chokes. This can be extended to some number of switches which is a positive integer power of two.

3. Dividing Transmission Line into N Parallel Transmission Lines with Switches

One way to provide transit-time isolation between switches is to place each switch in a separate transmission line. This delays the signal from a closing switch from reaching another switch by the transit time to get out of one transmission line plus that to reach the switch in a second one.

So as to present equal impedances to each switch let each of these N transmission lines have the same characteristic impedance(s). Using symmetry to give identical conditions for each gap we have C_N symmetry [5]. N-fold rotation axis). Assuming coaxial source and load transmission lines (O_2 symmetry) we have the geometry illustrated in Fig. 3.1. This also has N axial symmetry planes (C_{Na} symmetry).

Variations on this theme are also possible. The N transmission lines need not be straight. Using optical windows (perhaps with lenses) adjacent to each window, light (including ultraviolet) can be fed through each of the N transmission-line outer conductors to illuminate the other gaps, thereby making the early-firing gaps assist the closure of the remaining gaps.

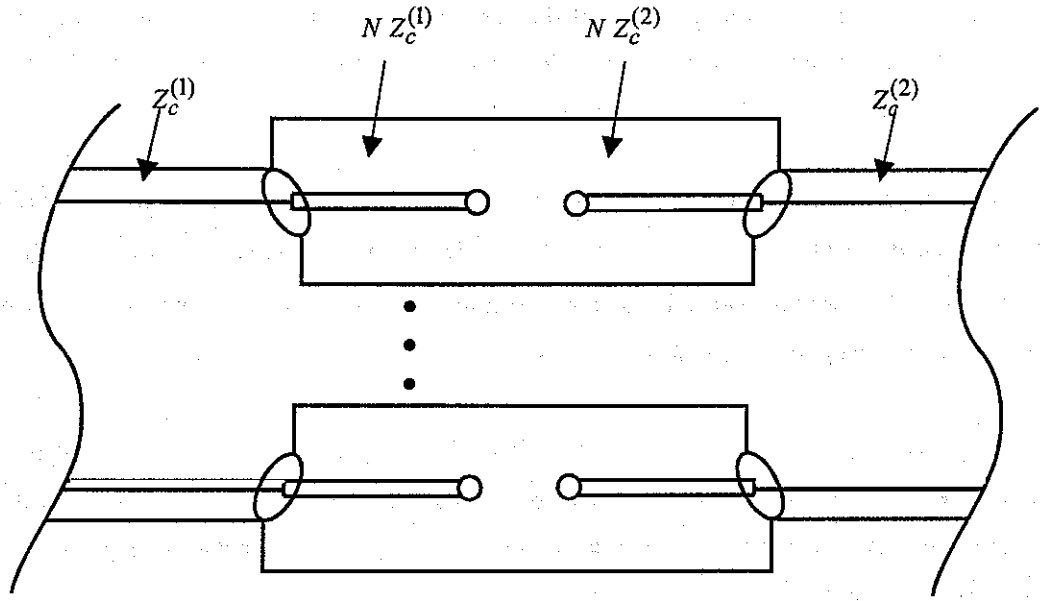

A. Side view

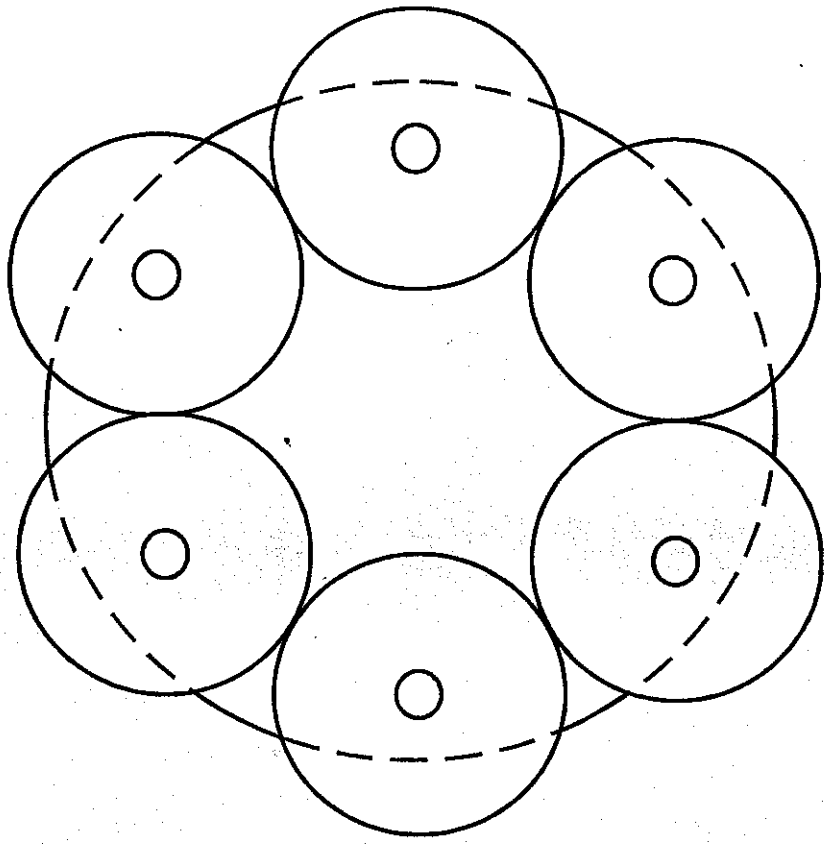

B. Corss-section view

Fig. 3.1 Divided Transmission Line for N Switches: Example for $N = 6$

4. Multichannel Switching in C_{Na} Geometry

Relaxing the requirement of N uncoupled transmission lines, let us consider N switches with some division of the source- and load-transmission-line center conductors. This brings in both transit-time and impedance-isolation concepts. Figure 4.1 shows an example of this in which slots are cut in the tubular center conductor to provide isolation of one switch-gap region (of N) from its nearest neighbors. Currents must flow around the slots, the slot length providing some transit time isolation. Of course, there is capacitive/inducting coupling across the slot (impedance isolation).

Also shown is a potential improvement by the addition of ferrite (or other magnetic material) *inside* the coaxial center conductor in the regions of the two sets of slots. One can think of this by considering the common mode (associated with all N switches firing) having a quasi uniform current density around the outside of the slotted cylinder with negligible magnetic field inside the cylinder to interact with the ferrite. Note the absence of ferrite near the slots to minimize interaction of the ferrite with the common mode. On the other hand if only one switch closes the current on that sector of the cylinder gives magnetic field both outside and inside the cylinder, the latter interacting with ferrite to increase the inductance presented to this current. However, the effect may not be large (say a factor of two). No ferrite should be on the outside of the cylinder as this would interfere with the common mode.

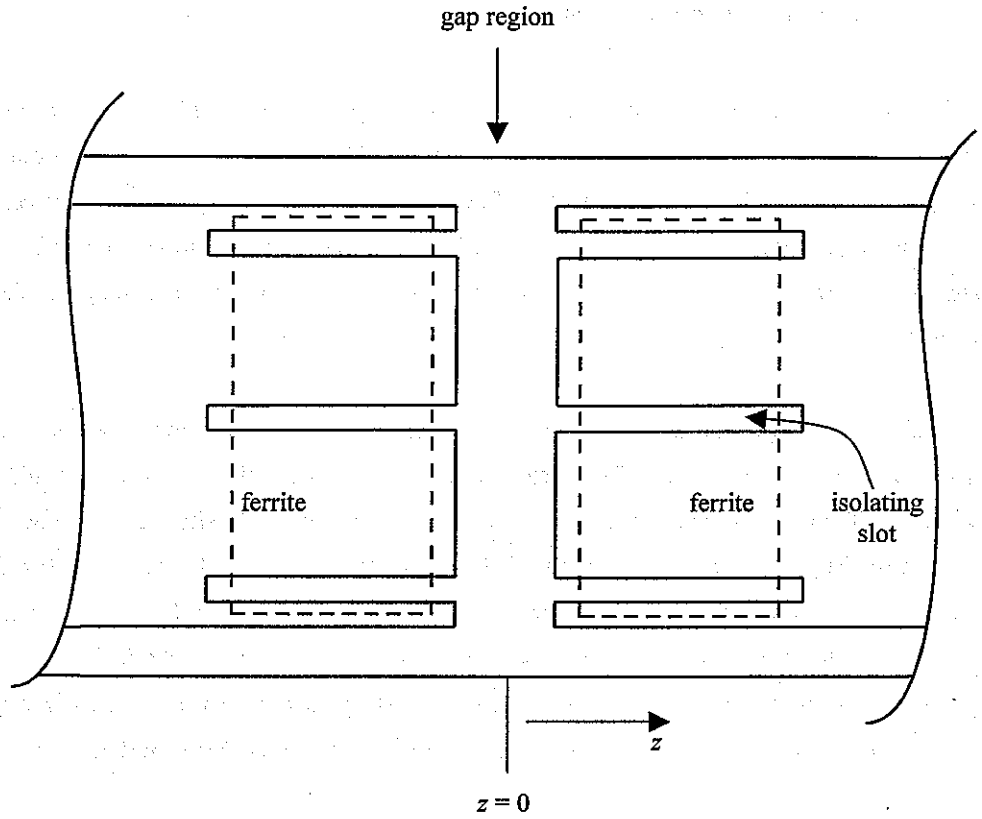

A. Side view

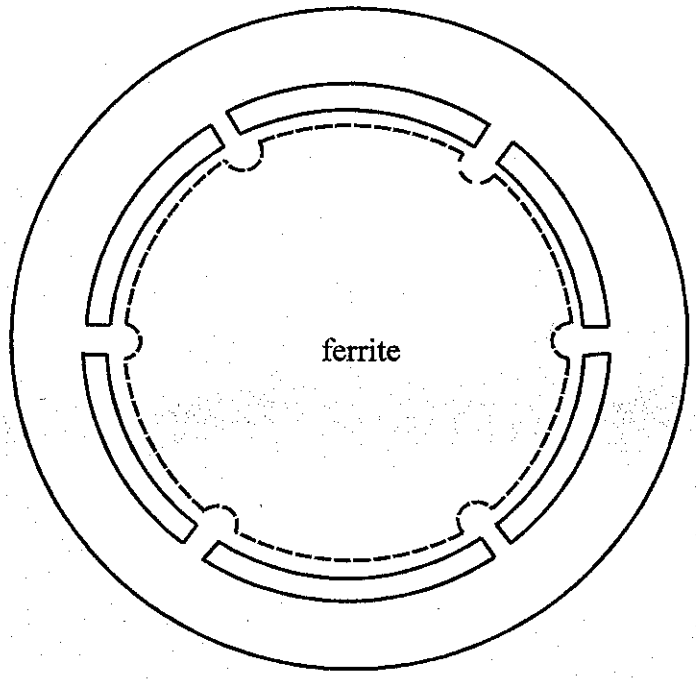

B. Cross section

Fig. 4.1 Multichannel Switch in C_{Na} Geometry: Example for $N = 6$.

5. Multiconductor Transmission Line with Switches in C_N Geometry

Consider the equivalent network in Fig. 5.1. On the left we have the source impedance matrix and open-circuit voltage sources. This gives voltages $\left(V_n^{(1)}\right) - \left(V_n^{(2)}\right)$ across the N switches with currents (I_n) through them into the load impedance matrix. Relating these variables we have

$$\left(\tilde{V}_n^{(2)}(s)\right) = \left(Z_{c_{n,m}}^{(2)}\right) \cdot \left(\tilde{I}_n(s)\right)$$

$$\left(\tilde{V}_n^{(1)}(s)\right) - \left(\tilde{V}_n^{(s)}(s)\right) = \left(\tilde{Z}_{n,m}^{(s)}(s)\right) \cdot \left(\tilde{I}_n(s)\right)$$

$$\left(\tilde{V}_n^{(1)}(s)\right) = \left(\tilde{V}_n^{(s)}(s)\right) - \left(Z_{c_{n,m}}^{(1)}(s)\right) \cdot \left(\tilde{I}_n(s)\right)$$

$$\left(Z_{c_{n,m}}^{(1)}\right) = \left(Z_{c_{n,m}}^{(1)}\right)^T \equiv \left(Y_{c_{n,m}}^{(1)}\right)^{-1} \equiv \text{source impedance matrix (real)}$$

$$\left(Z_{c_{n,m}}^{(2)}\right) = \left(Z_{c_{n,m}}^{(2)}\right)^T \equiv \left(Y_{c_{n,m}}^{(2)}\right)^{-1} \equiv \text{load impedance matrix (real)}$$

$$\left(\tilde{Z}_{n,m}^{(s)}(s)\right) = \begin{pmatrix} \tilde{Z}_1^{(s)}(s) & \cdots & 0 \\ \vdots & \ddots & \vdots \\ 0 & \cdots & \tilde{Z}_N^{(s)}(s) \end{pmatrix} = \left(\tilde{Y}_{n,m}^{(s)}(s)\right)^{-1} = \begin{pmatrix} \tilde{Y}_1^{(s)}(s) & \cdots & 0 \\ \vdots & \ddots & \vdots \\ 0 & \cdots & \tilde{Y}_N^{(s)}(s) \end{pmatrix}^{-1} \equiv \text{switch impedance matrix diagonal}$$

For convenience we define

$$\left(Z_{c_{n,m}}\right) = \left(Z_{c_{n,m}}^{(1)}\right) + \left(Z_{c_{n,m}}^{(2)}\right) = \left(Z_{c_{n,m}}\right)^T \equiv \left(Y_{c_{n,m}}\right)^{-1} \tag{5.2}$$

and we have

$$\begin{aligned} &\left(\tilde{V}_n^{(s)}(s)\right) = \left[\left(Z_{c_{n,m}}\right) + \left(\tilde{Z}_{n,m}^{(s)}(s)\right)\right] \cdot \left(\tilde{I}_n(s)\right) \\ &\left(\tilde{V}_n^{(g)}(s)\right) \equiv \left(\tilde{V}_n^{(1)}(s)\right) - \left(\tilde{V}_n^{(2)}(s)\right) = \left(\tilde{Z}_{n,m}^{(s)}(s)\right) \cdot \left[\left(Z_{c_{n,m}}\right) + \left(\tilde{Z}_{n,m}^{(s)}(s)\right)\right]^{-1} \cdot \left(\tilde{V}_n^{(s)}(s)\right) \\ &= \left[\left(1_{n,m}\right) + \left(Z_{c_{n,m}}\right) \cdot \left(\tilde{Y}_{n,m}^{(s)}(s)\right)\right]^{-1} \cdot \left(\tilde{V}_n^{(s)}(s)\right) \equiv \text{voltage vector across switch gaps} \end{aligned} \tag{5.3}$$

For present purposes the N-conductor transmission line is assumed lossless and nondispersive due to assumed perfect conductors embedded in a uniform dielectric medium with real, frequency-independent permittivity, ε, and permeability, μ (typically μ_0 as in free space). Then we have

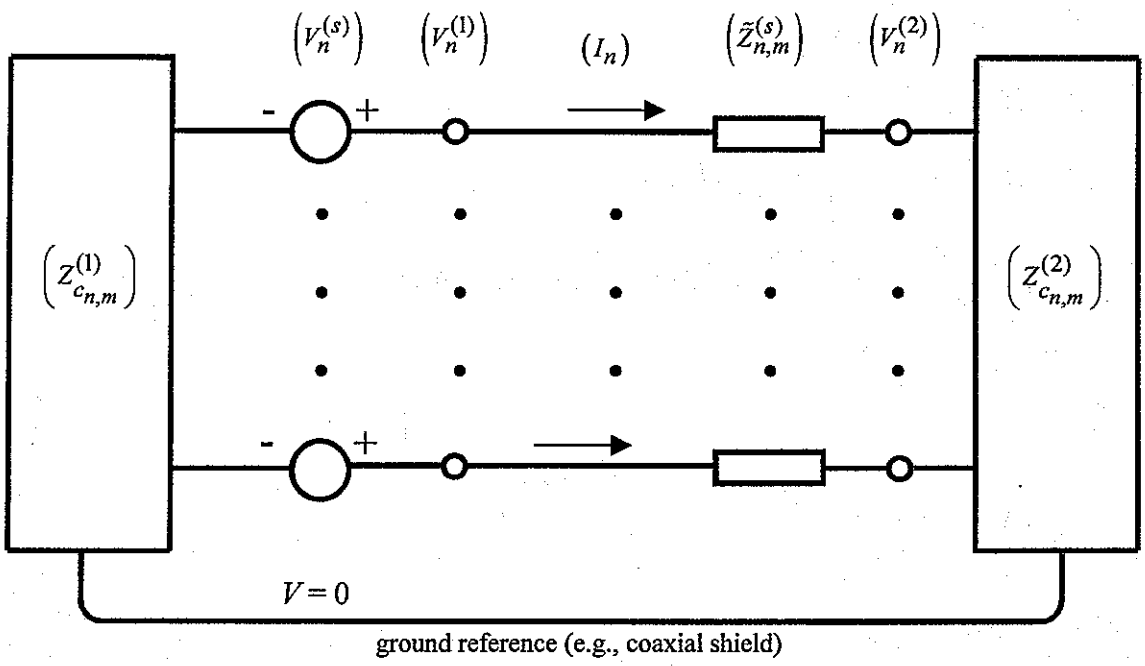

Fig. 5.1 Equivalent Circuit of N-Conductor (Plus Reference) Transmission Line with N Switch Gaps

$$Z_w \equiv \left[\frac{\mu}{\varepsilon}\right]^{\frac{1}{2}} \equiv Y_w^{-1} \equiv \text{ wave impedance}$$

$$\begin{aligned}
\left(Z^{(1)}_{c_{n,m}}\right) &= Z_w\left(f^{(1)}_{g_{n,m}}\right) \\
\left(Z^{(2)}_{c_{n,m}}\right) &= Z_w\left(f^{(1)}_{g_{n,m}}\right) \\
\left(Z_{c_{n,m}}\right) &= Z_w\left(f_{g_{n,m}}\right)
\end{aligned} \tag{5.4}$$

$$\left(f_{g_{n,m}}\right) = \left(f_{g_{n,m}}\right)^T = \left(f^{(1)}_{g_{n,m}}\right) + \left(f^{(2)}_{g_{n,m}}\right) \equiv \text{geometric-impedance-factor matrix (real)}$$

Note that here we have assumed the same dielectric medium on both sides of the switches, but this is not essential and Z_w can be appropriately superscripted if desired with little increase in complexity. Also note that all modes propagate with the same speed

$$\mathrm{v} = [\mu\varepsilon]^{-\frac{1}{2}} \leq \mathrm{c} = [\mu_0\varepsilon_0]^{-\frac{1}{2}} \tag{5.5}$$

Note that we have not yet assumed any geometrical symmetry for the transmission lines. We have assumed reciprocity. Then we have all eigenvalues of $(f_{g_{n,m}})$ real and nonnegative, and all eigenvectors constructable in real form.

Now consider the important special case

$\tilde{V}^{(s)}_N(s) = \tilde{V}^{(s)}_0(s) = Y$ (large (real) or even $\to \infty$)

$\tilde{V}^{(s)}_n(s) = 0$ for $n \neq N$ (open circuit)

Furthermore, let all the source voltages be the same corresponding to a voltage wave incident on the switches of amplitude V_0 as

$$\left(\tilde{V}^{(s)}_N(s)\right) = \frac{2V_0}{s}\begin{pmatrix}1\\ \vdots \\ 1\end{pmatrix}, \qquad \left(V^{(s)}_n(t)\right) = 2V_0u(t)\begin{pmatrix}1\\ 1\\ \vdots \\ 1\end{pmatrix} \tag{5.7}$$

The factor of 2 accounts for the +1 reflection from all open-circuited switches. The physical basis for all source voltages being the same concerns the common coaxial center conductor before it is slotted. Here the common conductor is assumed infinitely far away (far compared to transit times of interest). Then (5.3) takes the form

$$\left[\left(1_{n,m}\right) + \begin{pmatrix} & YZ_{c_{1,N}} \\ \bigcirc & \vdots \\ & YZ_{c_{N,N}} \end{pmatrix}\right] \cdot \left(V_n^{(g)}(t)\right) = 2V_0 u(t) \begin{pmatrix} 1 \\ \vdots \\ 1 \end{pmatrix} \tag{5.8}$$

Beginning with the Nth component we have

$$V_N^{(g)}(t) = \frac{2}{1+YZ_{c_{N,N}}} V_0 u(t) \to 0 \text{ as } Y \to \infty \tag{5.9}$$

Substituting this result in the equations for the remaining N-1 gap voltages gives for $n \neq N$

$$\begin{aligned} V_n^{(g)}(t) &= 2\left[1 - \frac{Y Z_{c_{n,N}}}{1+Y Z_{c_{N,N}}}\right] V_0 u(t) \\ &= 2\left[1 - \frac{Z_{c_{n,N}}}{Z_{c_{N,N}}}\right] V_0 u(t) \text{ as } Y \to \infty \\ &= 2\left[1 - \frac{f_{g_{n,N}}}{f_{g_{N,N}}}\right] V_0 u(t) \text{ as } Y \to \infty \end{aligned} \tag{5.10}$$

This gives the reduction in voltages on the remaining N-1 switches in terms of the elements of the geometric-impedance-factor matrix.

Now let us assume C_N symmetry on the two multiconductor transmission lines. Practically one may use C_{Na} symmetry but this does not add additional properties already given by reciprocity (C_{Nr} symmetry) [8]. This makes ($f_{g_{n,m}}$) not only circulant (row elements shifting to the right by one as one increases the row number by one), but bicirculant (same shifting property for columns) giving the general form

$$f_{n,m} = \text{function of } |n-m| \text{ only} \tag{5.11}$$

applying to all appearing in (5.4). C_N symmetry is defined in one representation by rotation matrices as

$$\begin{aligned} C_N &= \left\{ \begin{pmatrix} \cos(\phi_n) & -\sin(\phi_n) \\ \sin(\phi_n) & \cos(\phi_n) \end{pmatrix} \middle| n = 1, 2, \ldots, N \right\} \\ \phi_1 &= \frac{2\pi}{N}, \quad \phi_n = 2\pi\frac{n}{N}, \quad \phi_N = \phi_0 = 2\pi, \ 0 \end{aligned} \tag{5.12}$$

The identity (no rotation) is just $(C_N)_N = (C_N)_0$, i.e., the Nth (or 0th) element.

Summarizing from [3] we have for circulant matrices

$$\left(f_{n,m}\right) = \begin{pmatrix} f^{(1)} & f^{(2)} & \cdots & f^{(N)} \\ f^{(N)} & f^{(1)} & \cdots & f^{(N-1)} \\ \vdots & \vdots & & \vdots \\ f^{(2)} & f^{(3)} & \cdots & f^{(1)} \end{pmatrix} \tag{5.13}$$

$$f_\beta = \sum_{\ell=1}^{N} f^{(\ell+1)} e^{2\pi j \frac{\ell\beta}{N}} = \text{eigenvalues } (f_{N+1} = f_1)$$

Bicirculant matrices have, in addition,

$$f^{(\ell)} = f^{(N+2-\ell)} \tag{5.14}$$

and can be written as

$$\left(f_{n,m}\right) = \sum_{\ell=1}^{N} f_\beta \left(w_n\right)_\beta \left(w_n\right)_\beta \tag{5.15}$$

Note that bicirculant matrices are symmetric, and being real have real eigenvalue and can be constructed with real eigenvectors. Furthermore being positive semidefinite we have

$$f_\beta \geq 0 \text{ for } \beta = 1, 2, \ldots, N \tag{5.16}$$

Most eigenvalues are doubly degenerate. For N even we have

$$f_1 = f_{N-1}, \quad f_2 = f_{N-2}, \ldots, \quad f\frac{N}{2} - 1 = f\frac{N}{2} + 1 \tag{5.17}$$

with $F_{N/2}$ and f_N giving $N/2 + 1$ eigenvalues, and for N odd we have

$$f_1 = f_{N-1} \quad , \quad f_2 = f_{N-2} \quad , \quad \cdots, \quad f_{\frac{N-1}{2}} = f_{\frac{N+1}{2}} \tag{5.18}$$

with f_N giving $[N+1]/2$ eigenvalues

Note that

$$\left(f_{n,m}\right)^{\nu} = \sum_{\beta=1}^{N} f_{\beta}^{\nu}(w_n)_{\beta}(w_n)_{\beta} \tag{5.19}$$

and that the inverse of a bicirculant matrix is itself bicirculant (has same eigenvectors).

The eigenvectors take the form for the first "half"

$$(w_n)_{\beta} = \left[\frac{2}{N}\right]^{1/2} \begin{pmatrix} \cos\left(\frac{2\pi\beta}{N}\right) \\ \vdots \\ \cos\left(\frac{2\pi[N-1]\beta}{N}\right) \\ 1 \end{pmatrix}$$

$$\beta = \begin{cases} 1, 2, \ldots, \frac{N}{2} - 1 \text{ for } N \text{ even} \\ 1, 2, \ldots, \frac{N-1}{2} \text{ for } N \text{ odd} \end{cases} \tag{5.19}$$

$$\left(w_n\right)_{\frac{N}{2}} = N^{-1/2} \begin{pmatrix} -1 \\ +1 \\ -1 \\ \vdots \\ -1 \\ +1 \end{pmatrix} \text{ for } N \text{ even}$$

For $\beta = N$, or equivalently $\beta = 0$, we have

$$\left(w_n\right)_0 = \left(w_n\right)_N = \frac{1}{\sqrt{N}} \tag{5.20}$$

For the second "half" we have

$$(w_n)_{\beta} = \sqrt{\frac{2}{N}} \begin{pmatrix} \sin\left(\frac{2\pi\beta}{N}\right) \\ \vdots \\ \sin\left(\frac{2\pi[N-1]\beta}{N}\right) \\ 0 \end{pmatrix} \tag{5.21}$$

$$\beta = \begin{cases} \frac{N}{2} + 1, \frac{N}{2} + 2, \ldots, N - 1 \text{ for } N \text{ even} \\ \frac{N+1}{2}, \frac{N+3}{2}, \ldots, N-1 \text{ for } N \text{ odd} \end{cases}$$

For $\beta = N$, or equivalently $\beta = 0$, we have

$$(w_n)_0 = (w_n)_N = N^{-1/2}\begin{pmatrix}1\\ \vdots \\ 1\\ 1\end{pmatrix} \tag{5.22}$$

These modes have the general orthonormal property

$$(w_n)_{\beta_1} \cdot (w_n)_{\beta_2} = 1_{\beta_1,\beta_2} \tag{5.23}$$

For the bicirculant matrices which characterize our C_{Nr} symmetry, the computation of the eigenvalues and eigenmodes (eigenvectors) is considerably simplified.

6. Example of N Thin Wires in a Circular Cylinder with C_{Na} Geometry

As indicated in Fig. 6.1 let N wires, each of radius a, lie on a circular cylinder of radius $\Psi = \Psi_1$ in a cylindrical (Ψ, ϕ, z) coordinate system. These are in turn surrounded by a perfectly conducting surface on $\Psi = \Psi_2$. We assume that the wires are thin, i.e.,

$$a << \Psi_2 - \Psi_1 , \; 2\Psi_1 \sin\left(\frac{\phi_1}{2}\right) \tag{6.1}$$

so that we can solve the problem using line currents or charges. The wires are placed on $\phi = \phi_n$ where the ϕ_n are defined for C_N symmetry in (5.12). There are also N axial symmetry planes, but we do not use this fact.

For the self term (diagonal term in $(f_{g_{n,m}})$ or $f^{(1)}$) we consider the Nth (or 0th) wire on $\phi = 0$. Note the image wires located outside the conducting cylinder on $\Psi = \Psi_2^2/\Psi_1$. This is an example of reciprocation symmetry [9] and so we have given the image wires a similarly scaled (reciprocated) radius. However, these are replaced by line currents on Ψ_1 for purpose of analysis.

Of the various ways to solve this let us use the conformal transformation for two line charges or currents as in [1] with

$$\begin{aligned}
\zeta &= x + jy = \Psi e^{j\phi} \\
w &= u + jy = \ell n\left(\frac{\zeta - \Psi_3}{\zeta - \Psi_1}\right) \\
u &= \ell_n\left(\frac{|\zeta - \Psi_3|}{|\zeta - \Psi_1|}\right) = \frac{1}{2}\ell n\left(\frac{[x-\Psi_3]^2 + y^2}{[x-\Psi_1]^2 + y^2}\right) \\
\mathrm{v} &= \arg\left(\frac{\zeta - \Psi_3}{\zeta - \Psi_1}\right) \\
\Psi_3 &= \frac{\Psi_2^2}{\Psi_1} \equiv \text{image radius}
\end{aligned} \tag{6.2}$$

For convenience define a normalized parameter

$$\xi \equiv \frac{\Psi_1}{\Psi_2} = \frac{\Psi_2}{\Psi_3} > 1 \quad , \quad \xi^2 = \frac{\Psi_1}{\Psi_3} \tag{6.3}$$

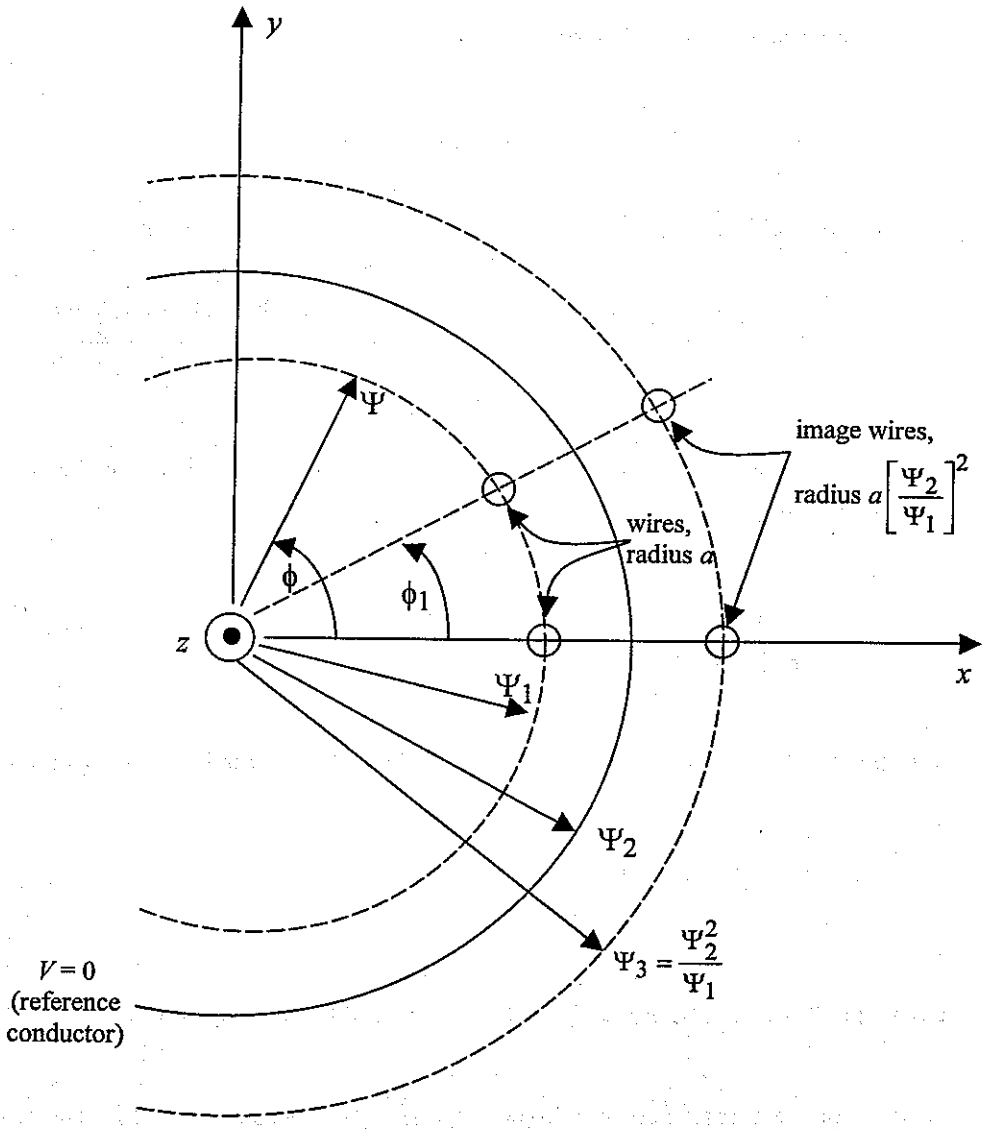

Fig. 6.1 Thin Wires in a Circular Cylinder with C_{Na} Symmetry

Rearrange the equation for u as

$$
\begin{aligned}
e^{u}\left[\left[x-\Psi_1\right]^2+y^2\right] &= e^{-u}\left[\left[x-\Psi_3\right]^2+y^2\right] \\
\left[e^{u}-e^{-u}\right]\left[y^2+x^2-2x\frac{\Psi_1 e^{u}-\Psi_1 e^{-u}}{e^{u}-e^{-u}}\right] &+ \Psi_1^2 e^{u}-\Psi_3^2 e^{-u}=0 \\
\left[x-\frac{\Psi_1 e^{u}-\Psi_3 e^{-u}}{e^{u}-e^{-u}}\right]^2 &+ y^2 = \left[\frac{\Psi_1 e^{u}-\Psi_3 e^{-u}}{e^{u}-e^{-u}}\right]^2 - \frac{\Psi_1 e^{u}-\Psi_3^2 e^{-u}}{e^{u}-e^{-u}}
\end{aligned}
\tag{6.4}
$$

This is the equation of a circle. So equipotentials (constant u) are circular cylinders. The circle of interest passes through $\zeta = \Psi_2 = x$ for which (6.2) gives

$$
u=\ell n\left(\frac{\Psi_3-\Psi_2}{\Psi_2-\Psi_1}\right) = -\ell n(\xi) \equiv u_c \tag{6.5}
$$

corresponding to $V = 0$ in our geometry. This equipotential surface is centered (from (6.4)) at

$$
\frac{\Psi_1 e^{u}-\Psi_3 e^{u}}{e^{u}-e^{-u}} = \frac{\Psi_1 \xi^{-1}-\Psi_3 \xi}{\xi-\xi^{-1}} = 0 \tag{6.6}
$$

with radius Ψ_2 as can be verified from the right side of the last equation in (6.4).

For the potential on wire N (or 0) we look at u close to $\zeta = \Psi_1$. Note that $\zeta = \Psi_1$ is technically the location of an equivalent line current or charge,. Based on the solution of a related problem [1], we can find by shifting the coordinate center to $\zeta = [\Psi_1 + \Psi_3]/2$, with effective centers at $\pm\,[\Psi_3 - \Psi_1]/2$, that a potential u_0 holds on a circular cylinder of radius a at

$$
\begin{aligned}
\frac{2a}{\Psi_3-\Psi_1} &= \operatorname{csch}(u_w) \equiv b = \frac{2a}{\Psi_2}\left[\xi+\xi^{-1}\right]^{-1} \\
u_w &= \operatorname{arccsch}(b) = \operatorname{arccsch}\left(\frac{2a}{\Psi_3-\Psi_1}\right) \\
&= \ell n\left(b^{-1}+\left[b^{-2}-1\right]^{1/2}\right)
\end{aligned}
\tag{6.7}
$$

So b is the appropriate normalized wire radius. For small b we have [6]

$$u_w = \ell n\left(\frac{2}{b}\right) + O\left(b^2\right) \text{ as } b \to 0 \tag{6.8}$$

The geometrical center of the wire $\Psi_1^{(g)}$ is a little to the left of the electrical center at

$$\begin{aligned} \Psi_1 - \Psi_1^{(g)} &= \frac{\Psi_3 - \Psi_1}{2}\left[\left[1+b^2\right]^{\frac{1}{2}} - 1\right] = \frac{\Psi_3 - \Psi_1}{2}\left[\frac{b^2}{2} + O\left(b^4\right)\right]^{\frac{1}{2}} \\ &= \frac{a^2}{\Psi_3 - \Psi_1}\left[1 + O\left(b^2\right)\right] \text{ as } b \to 0 \end{aligned} \tag{6.9}$$

which is negligible for sufficiently small b.

Noting that v changes by 2π in passing around the wire, and that the potential on the wire relative to the reference is $u_0 - u_c$ we have

$$\begin{aligned} f^{(1)} = f_{g_{n,n}} &= \frac{1}{2\pi}\left[\operatorname{arccsch}(b) - u_c\right] \\ &= \frac{1}{2\pi}\left[\operatorname{arccsch}(b) + \ell n(\xi)\right] \\ &= \frac{1}{2\pi}\left[\ell n\left(\frac{2}{b}\right) + \ell n(\xi)\right] + O\left(b^2\right) \text{ as } b \to 0 \\ &= \frac{1}{2\pi}\ell n\left(\frac{2\xi}{b}\right) + O\left(b^2\right) \text{ as } b \to 0 \end{aligned} \tag{6.10}$$

The other matrix elements are found by evaluating u at the locations of wires 1 through N-1, giving

$$\begin{aligned} u_n &= \frac{1}{2}\ell n\left(\frac{\left[\Psi_1\cos(\phi_n) - \Psi_3\right]^2 + \Psi_1^2\sin^2(\phi_n)}{\left[\Psi_1\cos(\phi_n) - \Psi_1\right]^2 + \Psi_1^2\sin^2(\phi_n)}\right) \\ &= \frac{1}{2}\ell n\left(\frac{\Psi_1^2 + \Psi_3^2 - 2\Psi_1\Psi_3\cos(\phi_n)}{2\Psi_3^2 - 2\Psi_1^2\cos(\phi_n)}\right) \\ &= \frac{1}{2}\ell n\left(\frac{\frac{1+\xi}{2} - \xi^{-2}\cos(\phi_n)}{1 - \cos(\phi_n)}\right) \end{aligned} \tag{6.11}$$

This translates to matrix elements

$$
\begin{aligned}
f^{(\ell)} &= f_{g_{n,m}} \quad \text{for } \ell = |n-m| + 1 \\
&= \frac{1}{2\pi}\left[\frac{1}{2}\ell n\left(\frac{\frac{1+\xi^{-4}}{2} - \xi^{-2}\cos(\phi_n)}{1 - \cos(\phi_n)}\right) + \ell n(\xi)\right] \\
&= \frac{1}{4\pi}\ell n\left(\frac{\frac{\xi^2 + \xi^{-2}}{2} - \cos(\phi_n)}{1 - \cos(\phi_n)}\right)
\end{aligned}
\tag{6.12}
$$

Noting that this is a function of ξ^2 we can write

$$
\begin{aligned}
\xi^2 &\equiv 1-p \quad , \quad \xi = [1-p]^{1/2} \\
\xi^{-2} &\equiv 1+p+p^2+\mathrm{O}\left(p^3\right) \text{ as } p \to 0 \\
\frac{\xi^2+\xi^{-2}}{2} &= 1+\frac{p^2}{2}+\mathrm{O}\left(p^3\right) \text{ as } p \to 0
\end{aligned}
\tag{6.13}
$$

we have

$$
\begin{aligned}
f^{(\ell)} &= \frac{1}{4\pi}\ell n\left(1+\frac{1}{2}\frac{p^2}{1-\cos(\phi_n)} + \mathrm{O}\left(p^3\right)\right) \\
&= \frac{1}{8\pi}\frac{p^2}{1-\cos(\phi_n)} + \mathrm{O}\left(p^3\right)
\end{aligned}
\tag{6.14}
$$

This gives us enough to be able to calculate the modal eigenvalues discussed in Section 5, if desired. These apply to each of the geometric-impedance-factor matrices. Similarly expanding $f^{(1)}$ for small p we have

$$
\begin{aligned}
f^{(1)} &= \frac{1}{2\pi}\left[\operatorname{arccsch}(b) + \frac{1}{2}\ell n(1-p)\right] \\
&= \frac{1}{2\pi}\left[\operatorname{arccsch}(b) - \frac{p}{2} + \mathrm{O}\left(p^2\right)\right] \text{ as } p \to 0 \\
&= \frac{1}{2\pi}\left[\ell n\left(\frac{2}{b}\right) - \frac{p}{2}\right] + \left[\mathrm{O}\left(b^2\right) \text{ as } b \to 0\right] + \left[\mathrm{O}\left(p^2\right) \text{ as } p \to 0\right]
\end{aligned}
\tag{6.15}
$$

Now we are in a position to evaluate the voltage on the switch gaps assuming that number N (or 0) is shorted as in (5.10). The above results can be used to evaluate the matrix elements as

$$f^{(1)} = f^{(1,1)} + f^{(1,2)} = \frac{1}{2\pi}\left[\operatorname{arccsch}\left(b^{(1)}\right) + \operatorname{arccsch}\left(b^{(2)}\right) - \ell n\left(\xi^{(1)}\right) - \ell n\left(\xi^{(2)}\right)\right]$$

$$= \frac{1}{2\pi}\left[\ell n\left(\frac{2}{b^{(1)}}\right) + \ell n\left(\frac{2}{b^{(2)}}\right) - \frac{p^{(1)}}{2} - \frac{p^{(2)}}{2}\right]$$

$$+ O\left(b^{(1)^2}\right) + O\left(b^{(2)^2}\right) + O\left(p^{(1)^2}\right) + O\left(p^{(2)^2}\right)$$

as these four parameters $\rightarrow 0$

$$f^{(\ell)} = \frac{1}{4\pi}\left[\ell n\left(\frac{\frac{\xi^{(1)^{-2}} + \xi^{(1)^2}}{2} - \cos(\phi_n)}{1 - \cos(\phi_n)}\right) + \ell n\left(\frac{\frac{\xi^{(2)^{-2}} + \xi^{(2)^2}}{2} - \cos(\phi_n)}{1 - \cos(\phi_n)}\right)\right] \tag{6.16}$$

$$= \frac{1}{8\pi}\,\frac{p^{(1)^2} + p^{(2)^2}}{1 - \cos(\phi_n)} + O\left(p^{(1)^3}\right) + O\left(p^{(2)^3}\right)$$

as these two parameters $\rightarrow 0$

where the additional superscripts 1 and 2 apply respectively to the parameters to the left (negative z) and right (positive z) as in Fig. 4.1.

The fractional voltage reduction in (5.10) can then be expressed as

$$\frac{f_{g_{n,N}}}{f_{g_{N,N}}} = \frac{f^{(\ell)}}{f^{(1)}} \quad \text{for} \quad \ell \geq 2 \tag{6.17}$$

For small parameters as in (6.15) this is

$$\frac{f^{(\ell)}}{f^{(1)}} = \frac{1}{4}\,\frac{p^{(1)^2} + p^{(2)^2}}{1 - \cos(\phi_n)}\left[\ell n\left(\frac{2}{b^{(1)}}\right) + \ell n\left(\frac{2}{b^{(2)}}\right) - \frac{p^{(1)}}{2} - \frac{p^{(1)}}{2}\right] + \cdots \tag{6.18}$$

As we would like this ratio to be small we can see that wires farther from the shorted gap (smaller $\cos(\phi_n)$) have the least voltage reduction. The largest reduction occurs for the nearest neighbor gaps with $n = 1, N-1$. Moving the wires closer to the conducting circular cylinders (reference conductors) reduces both $p^{(1)}$ and $p^{(2)}$ lowering the above ratio for all switch gaps (except $n = N$, the shorted gap). Similarly lowering wire radii and hence $b^{(1)}$ and $b^{(2)}$, also lowers the reduction factor, but only logarithmically. The normalized voltage on the nearest neighbor to the $n = N$ (or 0) wire is now

$$
\begin{aligned}
v_1 &= v_{N-1} = 1 - \frac{f^{(2)}}{f^{(1)}} \\
&= 1 - \frac{1}{2}\frac{\left(\ell n \dfrac{\xi^2 + \xi^{-2} - \cos(\phi_1)}{1 - \cos(\phi_1)}\right)}{\operatorname{arccsch}(b) + \ell n(\xi)} \\
&= 1 - \frac{1}{2}\frac{\ell n\left(\dfrac{\xi^2 + \xi^{-2} - \cos(\pi/N)}{1 - \cos(\pi/N)}\right)}{\operatorname{arccsch}(b) + \ell n(\xi)}
\end{aligned}
\tag{6.19}
$$

For the reader's benefit we also have the common-mode impedance of the N-conductor system (plus reference conductor), as this is the impedance of the source or load by appropriate introduction of the 1 and 2 superscripts. Writing this in normalized form we have

$$
f_{com} = \frac{Z_{com}}{Z_w} = \frac{1}{N} \quad \text{[eigenvalue for common mode]}
$$

$Z_{com} \equiv$ common-mode impedance (equal voltages on all wires, equal currents in all wires)

$$
\begin{aligned}
f_{com} &= \frac{1}{N}\sum_{\ell=0}^{N-1} f^{(\ell)} \\
&= \frac{1}{2\pi N}\left[\operatorname{arccsch}(b) + \ell n(\xi) + \frac{1}{2}\sum_{n=1}^{N-1} \ell n\left(\frac{\dfrac{\xi^2 + \xi^{-2}}{2} - \cos\left(\dfrac{2\pi n}{N}\right)}{1 - \cos\left(\dfrac{2\pi n}{N}\right)}\right)\right]
\end{aligned}
\tag{6.20}
$$

The factor of $1/N$ comes from summing the N identical currents on the N wires.

The reader should note that there are limitations on the range of validity of these formulae. First the wires for $n = 1, \ldots, N-1$ should not be too close to their images, or equivalently to the reference cylinder, implying

$$
a << \Psi_2 - \Psi_1 \quad , \quad b << \frac{\Psi_2 - \Psi_1}{\Psi_1} = \xi^{-1} - 1 \tag{6.21}
$$

Second the wires should not be too close to each other implying

$$
\begin{aligned}
2a &<< \Psi_1 \; 2 \sin\left(\frac{\phi_1}{2}\right) \simeq \Psi_1 \phi_1 \quad \text{for large } N \\
b &<< \frac{2\Psi_1}{\Psi_3 - \Psi_1}\sin\left(\frac{\pi}{N}\right) = 2\left[\xi^{-2} - 1\right]^{-1}\sin\left(\frac{\pi}{N}\right) \simeq \frac{2\pi}{N}\left[\xi^{-2} - 1\right] \quad \text{for large } N
\end{aligned}
\tag{6.22}
$$

These in turn limit the range of applicability of ξ as

$$[b + 1]^{-1} >> \xi >> \left[\frac{2\sin\left(\frac{\pi}{N}\right)}{b} + 1\right]^{-1/2} \simeq \left[\frac{Nb}{2\pi}\right]^{1/2} \text{ for large } N \tag{6.23}$$

To illustrate these results and get some feel for the effects of varying the normalized parameters (normalized wire radius b, and normalized radius of wire location ξ) some numerical computations are plotted in Figs. 6.2-4. Each of these figures corresponds to a separate value of b (0.02, 0.05, 0.1). Each figure has three parts. Part A has v_1 as a function of ξ with $N = 2, 4, 6, 8$ as a parameter. The interesting region near $\xi = 1$ for which v_1 approaches 1 (good isolation) is depicted as $1 - v_1$ in part B with a vertical logarithmic scale. Part C plots $N f_{com}$ as a function of ξ with N as a parameter, including $N = 1$. Note that in this form all the curves come together as $\xi \to 1$. Note that (6.22) restricts the range of ξ near $\xi = 1$. A factor of two is taken on the allowed range of ξ based on the left side of the equation.

As $\xi \to 1$ each wire is dominantly associated with the circular cylinder defining $V = 0$, the mutual terms (ϕ_1 through ϕ_N) being comparatively negligible. This is the case of good isolation between the wires (one switch firing negligibly affecting the adjacent switches. For smaller values of ξ we can see the effect of the mutual interaction, particularly as N is increased. Note that the dependence on b is slight (roughly logarithmic).

While we have illustrated the case for $\left(Z^{(1)}_{c_{n,m}}\right) = \left(Z^{(2)}_{c_{n,m}}\right)$ (left and right multiconductor systems identical), the numbers are still valid as long as $\left(Z^{(2)}_{c_{n,m}}\right)$ is a positive scalar multiple of $\left(Z^{(1)}_{c_{n,m}}\right)$. This is due to the normalized way of defining v_1. So, for example, the left side could have a much lower characteristic impedance than the right side), giving a voltage increase on passing through the switches. However, to achieve this simple case, one will in general have a shift in radial position between wires connected to the same switch. Of course, one may return to (6.15) and have different ξ and b values, as well as the radii of left and right reference cylinders, as one wishes and compute the appropriate $f^{(1)}$ and $f^{(2)}$ to use (6.18).

The reader can find some related material for this geometry in [7].

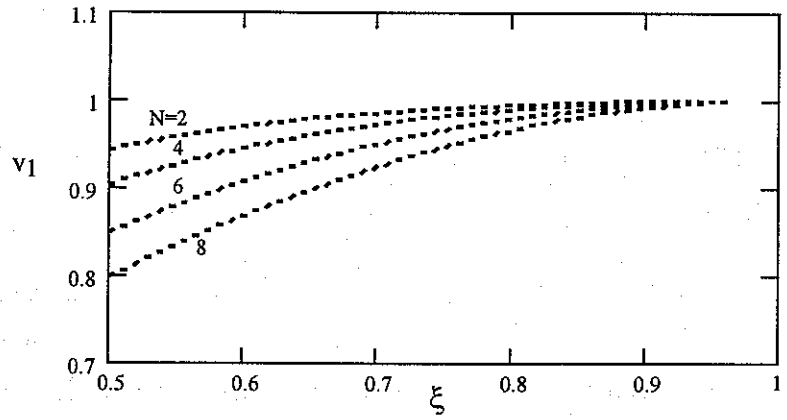

A. Normalized voltage on switch gap adjacent to shorted gap.

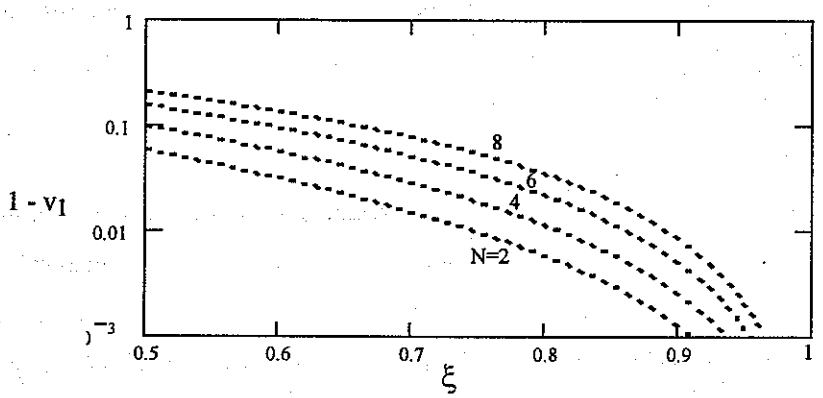

B. Expansion of $1-v_1$ near $v_1=1$.

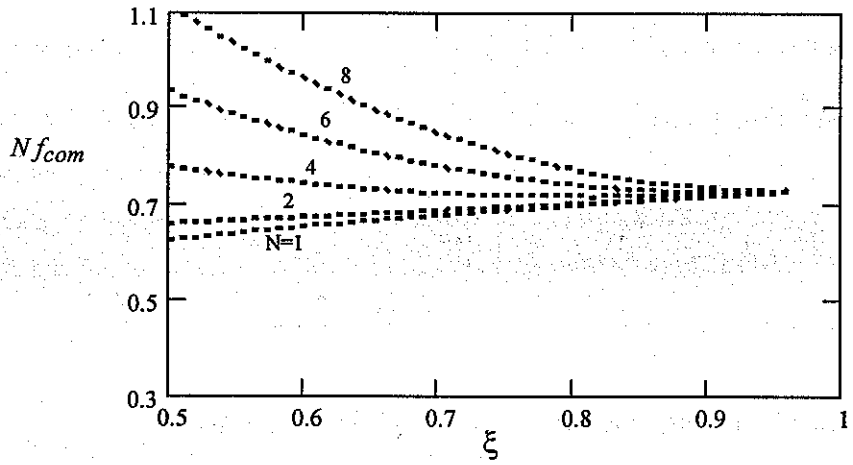

C. Geometric factor in common mode impedance.

Fig. 6.2 Voltage Reduction on Switch Gap Adjacent to Shorted Gap: $b = 0.02$.

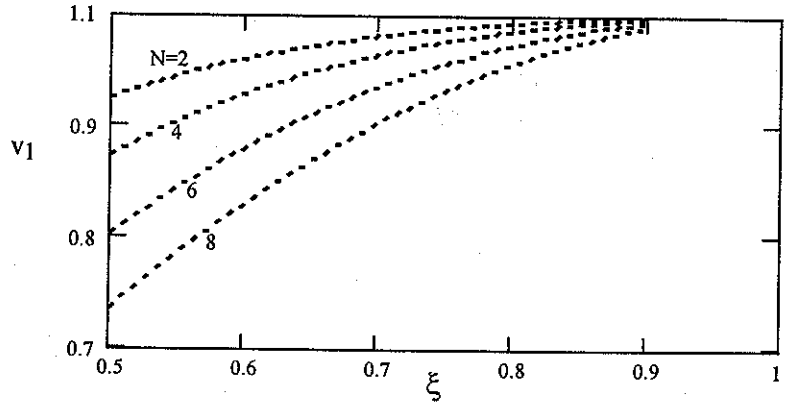

A. Normalized voltage on switch gap adjacent to shorted gap.

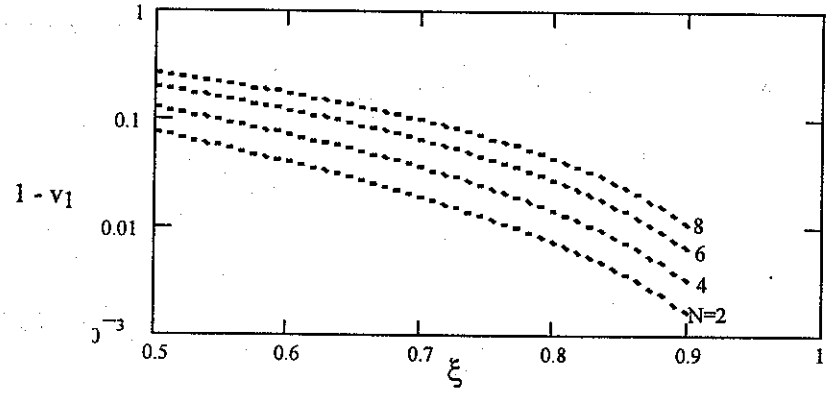

B. Expansion of 1-v_1 near v_1=1.

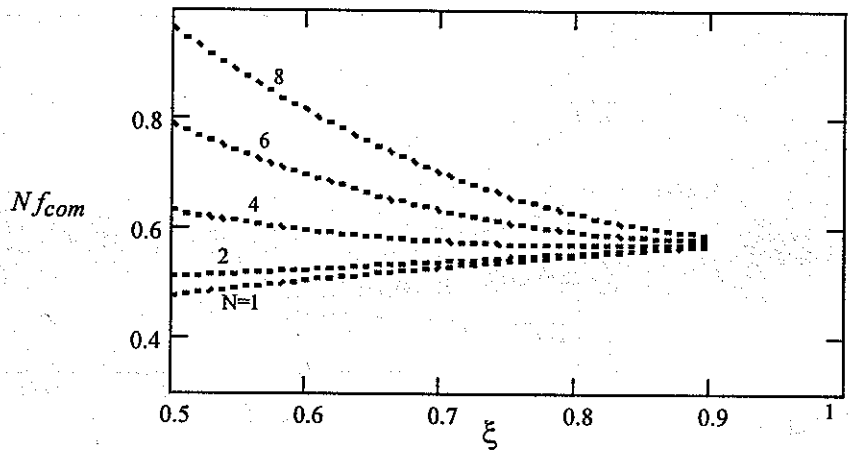

C. Geometric factor in common mode impedance.

Fig. 6.3 Voltage Reduction on Switch Gap Adjacent to Shorted Gap: $b = 0.05$.

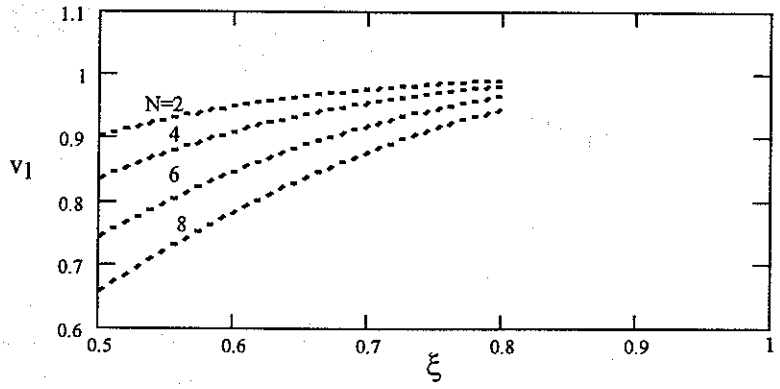

A. Normalized voltage on switch gap adjacent to shorted gap.

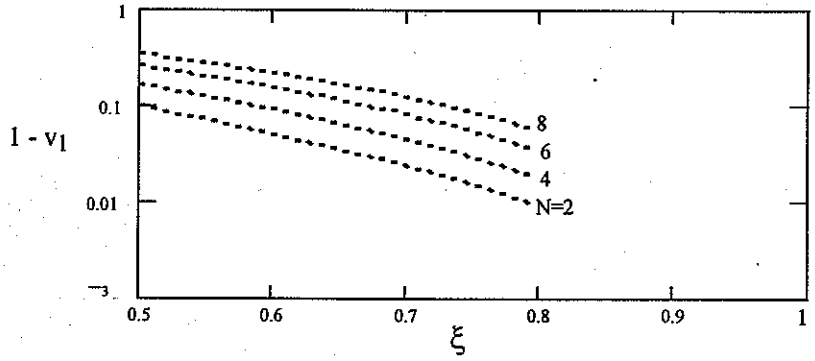

B. Expansion of $1-v_1$ near $v_1=1$.

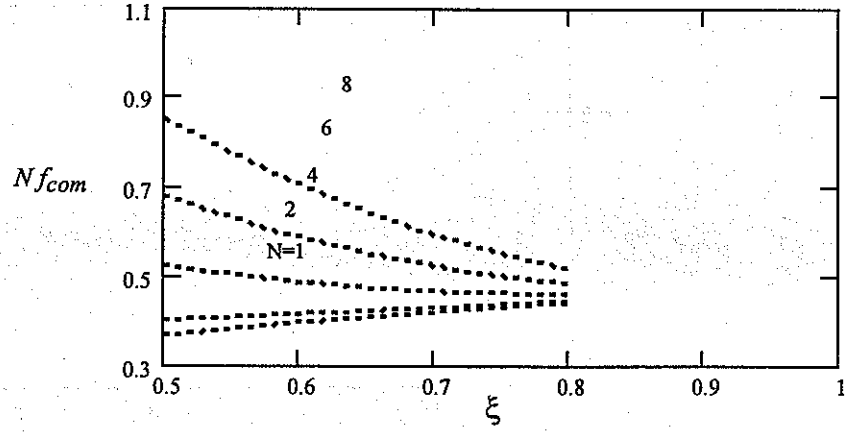

C. Geometric factor in common mode impedance.

Fig. 6.4 Voltage Reduction on Wwitch Gap Adjacent to Shorted Gap: $b = 0.1$.

7. Concluding Remarks

This paper considers some of the electromagnetic aspects of multichannel switching. Various techniques have been described for isolating (in various degrees) one switch gap from another based on transit-time isolation and/or reduction of mutual coupling (impedance isolation). These results can, of course, be extended by more detailed calculations. Note that we have not considered the nonlinear/statistical problem of the actual closure of the individual switches.

References

1. C. E. Baum, "Impedances and Field Distributions for Symmetrical Two Wire and Four Wire Transmission Line Simulators", Sensor and Simulation Note 27, October 1966.

2. C. E. Baum, "Transient Arrays", Sensor and Simulation Note 392, February 1996; pp. 129-138, in C. E. Baum, L. Carin, and A. P. Stone (eds.), *Ultra-Wideband, Short-Pulse Electromagnetics 3*, Plenum, 1997.

3. J. Nitsch, C. E. Baum, and R. Sturm, "The Treatment of Commuting Nonuniform Tubes in Multiconductor-Transmission-Line Theory", Interaction Note 481, May 1990.

4. J. C. Martin, "Multichannel Gaps", Switching Note 10, march 1970; Section 10c, pp. 295-333, in T. H. Martin, A. H. Guenther, and M. Kristiansen (eds.), *J. C. Martin on Pulsed Power*, Plenum, 1996.

5. C. E. Baum, "Combining RF Sources Using C_N Symmetry", Circuit and Electromagnetic System Design Note 37, June 1989.

6. H. B. Dwight, *Tables of Integrals and Other Mathematical Data*, Macmillan, 1961.

7. S. Frankel, "Cable and Multiconductor Transmission Line Analysis", HDL-TR-091-1, June 1974; *Multiconductor Transmission Line Analysis*, Artech House, 1977.

8. C. E. Baum and H. N. Kritikos, "Symmetry in Electromagnetics", ch. 1, pp. 1-90, in C. E. Baum and H. N. Kritikos, *Electromagnetic Symmetry*, Taylor & Francis, 1995.

9. E> G. Farr and C. E. Baum, "Radiation From Self-Reciprocal Apertures", ch. 6, pp. 281-308, in C. E. Baum and H. N. Kritikos (eds.), *Electromagnetic Symmetry*, Tayl,or & Francis, 1995.